

# Self-deployable *origami* stent grafts as a biomedical application of Ni-rich TiNi shape memory alloy foil

Kaori Kuribayashi<sup>a,\*</sup>, Koichi Tsuchiya<sup>b</sup>, Zhong You<sup>a</sup>, Dacian Tomus<sup>b</sup>,  
Minoru Umemoto<sup>b</sup>, Takahiro Ito<sup>c</sup>, Masahiro Sasaki<sup>c</sup>

<sup>a</sup> Department of Engineering Science, University of Oxford, Parks Road, Oxford OX1 3PJ, UK

<sup>b</sup> Department of Production Systems Engineering, Toyohashi University of Technology, Toyohashi, Aichi 441-8580, Japan

<sup>c</sup> Nippon Metal Industry, Co., Ltd., Sagamihara, Kanagawa 229-1184, Japan

Received in revised form 2 December 2005; accepted 2 December 2005

## Abstract

This paper describes the design, manufacturing and properties of a new type of stent graft, the origami stent graft. Unlike conventional stent grafts which consist of a wire mesh stent and a covering membrane, the new origami stent graft is made from a single foldable foil with hill and valley folds. The Ni-rich titanium/nickel (TiNi) shape memory alloy (SMA) foil made by the newly developed ultrafine laminates method was used in order to produce the stent graft. The pattern of folds on the foil was produced by negative photochemical etching. The deployment of the stent graft is achieved either by SMA effect at the body temperature or by making use of property of superelasticity. A number of prototypes of the stent graft, which are the same size as standard oesophageal and aortal stent grafts, have been produced successfully. It was demonstrated that the stent graft deploy as expected.

© 2006 Elsevier B.V. All rights reserved.

**Keywords:** Stent graft; Self-deployable structure; Ni-rich TiNi SMA foil; Photochemical etching

## 1. Introduction

A stent is a type of flexible tubular device and is capable of being folded to fit into small dimensions for minimum invasive surgery. It is then deployed to open up a blocked lumen and also to protect a weakened lumen in the human body. It is widely used in the treatment of diseases such as coronary artery stenosis, aortic aneurysm or oesophageal cancer [1–4]. There are two types of stents: stents and stent grafts. Most current stents have a mesh structure, whereas a stent graft is composed of a deployable wire mesh stent and a soft covering membrane (graft).

One of the major problems of current stents is restenosis, that is, the blocking of the once opened lumen due to tissue in-growth through the openings of the meshes [5,6]. Stent grafts have been developed as an effective way to prevent restenosis by their graft cover. However, it was reported problems of wire mesh fractures and graft ruptures [7,8]. It is probably due to

a geometric incompatibility between the stent and graft when their deployment because the graft is simply attached the mesh stent.

In a previous research, a new single piece stent graft was developed to improve the structural design of currently available stent grafts [9]. The new stent graft has an integrated enclosure without additional covering, therefore preventing tissue in-growth. In addition, it does not have the incompatibility problem between mesh stent and graft during its deployment.

Fig. 1(a and b) show the photographs of one of the new stent graft designs made from a single sheet of card in its fully folded and deployed configurations, respectively. The folding of the new stent graft is achieved by dividing a cylindrical tube into a series of identical elements with hill and valley folds as in origami. Fig. 1(c) shows the pattern of folds. The solid and broken lines represent hill and valley creases, respectively. The folds act as hinges when the stent graft is folded. One of the interesting properties of the folding pattern is that it causes the stent graft to fold and deploy both longitudinally and radially. Therefore, the diameter and length decrease and increase when they fold and deploy, respectively. In addition, the folded configuration of each element also makes the stent graft flexible. These

\* Corresponding author. Tel.: +44 1865 273137; fax: +44 1865 283301.

E-mail address: kaori.kuribayashi@st-catherines.oxon.org (K. Kuribayashi).

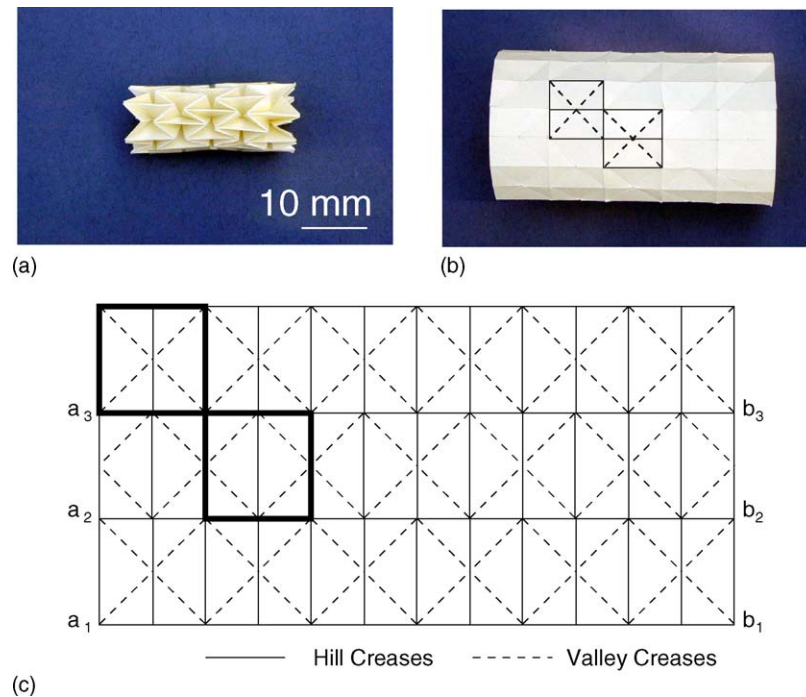


Fig. 1. Photographs of a card model of the origami stent graft in its (a) fully folded, (b) deployed configurations and (c) deployment of the folding pattern. The opposite edge of a sheet,  $a_1$ - $a_2$ - $a_3$  and  $b_1$ - $b_2$ - $b_3$  are joined together to form a cylindrical tube.

properties are suitable for the stent graft design because it can be packaged compactly and ensure flexibility when folded. The new stent graft is named *origami* stent graft since the paper folding patterns used in the Japanese art of origami are employed to fold the stent graft.

TiNi SMA have already been used in stent graft applications [10] because of its shape memory effect [11], as well as its biocompatibility [12,13]. The SMA stent graft is packed inside a sheath so that it can be passed through a narrow space. Once it reaches the intended site, the sheath is withdrawn and the stent graft deploys. Difference between existing SMA stent grafts and origami stent graft the latter is made using a foil instead of wires. Compared to the wire forms, usage of SMA foils is very limited. Complex rolling and annealing methods are required to produce a large and thin foil because of the low plastic workability and high work hardening rate of SMA. Therefore, commercially available SMA foils are still very expensive, resulting in the rarity of SMA foils in industrial products. A new method has recently been developed to produce the foil using ultrafine laminates of pure Ti and Ni [14], which can reduce the cost. This improvement to the production of SMA foils is expected to lead to a significant expansion in the number of applications of SMA.

This paper is organized as follows. Section 2 introduces a new Ni-rich TiNi SMA foil for the origami stent graft. In Section 3, process methods of producing the stent graft including photochemical etching and heat-treatment are described. Etching was used to produce grooves of folds. Heat-treatment was given after etching to store a memory of a cylindrical shape for the stent graft. In Section 4, we demonstrate the self-deployment of the origami stent graft at near body temperature. In addition

mechanical property of the stent graft in fully deployed configuration is measured. The conclusions are summarized in Section 5.

## 2. Material

In this research, two different Ni-rich TiNi SMA foils (Ti–50.7 at% Ni or Ti–51.3 at% Ni) were used in order to produce self-deployable origami stent grafts at body temperature triggered either thermally or mechanically. One is expected to deploy by heating. The other is expected to deploy due to the property of superelastic behaviour of SMA. It is recovered the original deployed configuration of the stent graft on a reduction of stress after the sheath which covers the stent graft is withdrawn.

The foils were produced by a method in which a diffusion treatment (at 1073 K for 72 h) was carried out to the ultrafine laminates foils composed of alternative layers of pure Ti (about 700 nm in thickness) and pure Ni (about 200 nm in thickness). One of the advantages of this TiNi SMA foil is that the foils do not have a rolling direction because the new process does not require rolling, which also reduces manufacturing cost. Detail of this method and properties of the material are given by Tomus et al. [14].

In the present study, Ni-rich TiNi foils were used because martensitic transformation temperature is adjustable to the temperature near human body by appropriate aging. Transformation temperature is very sensitive for the amount of Ni [15,16]. Therefore, the transformation temperature of the Ni-rich TiNi SMA foils with Ti–50.7 at% Ni and Ti–51.3 at% Ni will be different after aging treatment.

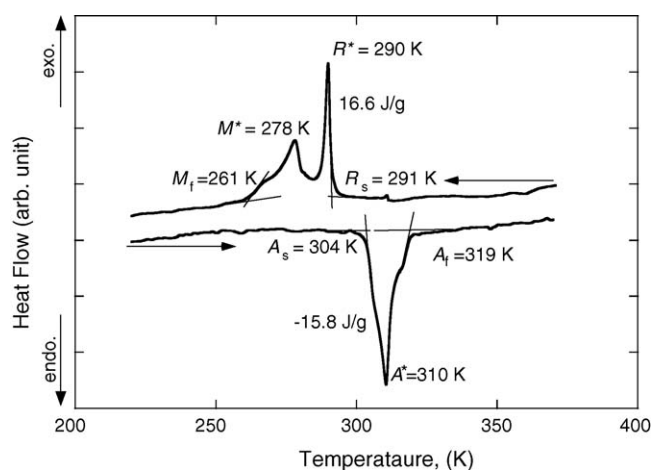


Fig. 2. DSC profile of Ti–50.7 at% Ni foil after diffusion treatment at 1073 K for 72 h and aging at 773 K for 40 h.

The aging treatment at 773 K for 20–40 h for foils was done in order to set the transformation temperature close to body temperature. The transformation temperature was measured by differential scanning calorimetry (DSC) with a cooling/heating rate of  $0.17 \text{ K s}^{-1}$ . Fig. 2 shows a result of a DSC profile for the Ti–50.7 at% Ni foil after diffusion and aging (at 773 K, 40 h) treatments. There are two transformation peaks on cooling and one on heating. On cooling the first peak,  $R^*$  at 290 K, and second one,  $M^*$  at 278 K can be assigned for B2 to R transformation and R to B19' transformation temperatures, respectively. Transformation temperatures are determined as  $R_s = 291 \text{ K}$ ,  $R^* = 290 \text{ K}$ ,  $M^* = 278 \text{ K}$ ,  $M_f = 261 \text{ K}$ ,  $A_s = 304 \text{ K}$ ,  $A^* = 310 \text{ K}$ , and  $A_f = 319 \text{ K}$ . Here  $R_s$ ,  $M_{s,f}$ , and  $A_{s,f}$  carry their standard meaning, and '\*' indicates the peak temperature for the corresponding transformation. Therefore, shape memory recovery will occur near body temperature (about 310 K). Similar measurement has been done for the Ti–51.3 at% Ni foil after diffusion aging (at 773 K for 20 h) treatments. Transformation temperatures ( $R_s = 295 \text{ K}$ ,  $R^* = 286 \text{ K}$ ,  $M^* = 262 \text{ K}$ ,  $M_f = 239 \text{ K}$ ,  $A_s = 293 \text{ K}$ ,  $A^* = 305 \text{ K}$ , and  $A_f = 312 \text{ K}$ ) are lower than those for the Ti–50.7 at% Ni foil. Thus, this foil is superelastic at near body temperature.

### 3. Manufacture of the origami stent graft

#### 3.1. Etching process for producing folds

The Ni-rich TiNi SMA foils ( $50 \text{ mm} \times 100 \text{ mm} \times 0.05 \text{ mm}$ ) were etched to create grooves for the folds of the origami stent graft using a negative photochemical etching process. Etching is less expensive and offers a finer control over the etching depth so that precise and complex designs will be produced in comparison with other processing methods including laser cutting, electro-discharged machining [17,18]. The advantages of negative etching are that the etching process is easier and cheaper than positive etching process. Furthermore, uniform coating can be applied over a large area using a negative photoresist, which would become particularly important in the large scale manufacture of stent grafts.

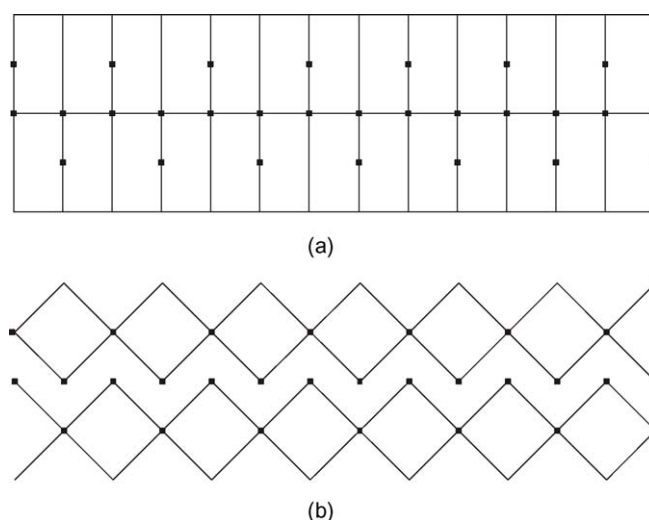


Fig. 3. Folding pattern of the self-deploying origami stent graft (a) outer and (b) inner surfaces.

Fig. 3(a and b) show the pattern of folds for the front and reverse sides of the foil, which correspond to the hill and valley creases of the origami stent graft (see Fig. 1). The width of the grooves is 0.3 mm. The sizes of square elements and central holes are 10 and 0.5 mm, respectively. The numbers of elements in both vertical and longitudinal directions are 8 and 4, respectively. The holes are matched up on the front and reverse sides of the foil, so that they become through-holes after etching. The holes help to alleviate high concentrations of stress when the foil is folded.

The etching process is as follows. Firstly, the foil was coated with either single or double layers (0.035 or 0.070 mm in thickness) of a negative dry photoresist (Riston 205, Dupont Co.). Secondly, the coated foil was exposed to a 2 kW UV source for 15 s. Thirdly, it was developed in a 1% solution of potassium carbonate, and then baked at 363 K for 30 min. Finally, both sides of the foil were etched at the same time with an etchant which contains mixed solutions of HF/HNO<sub>3</sub>/H<sub>2</sub>O in the proportion of 1:1:6 by volume. The thickness of the foil was halved at the folds by the etching process.

It was found that during the negative etching process, single dry photoresist of 0.035 mm in thickness peeled off immediately. It was not resistant enough to adhere to the SMA foil. We therefore used a double-coated photoresist was able to withstand the etching process.

Fig. 4 shows the photographs of the TiNi foil after etching the folding pattern. Good folding patterns were produced. The total etching time to reduce the thickness to half of its initial value was 16 min. In general, when etching a metal using a liquid etchant, it is etched not only in the depth direction, as desired, but also to the side, which results in the formation of a sidewall under the photoresist known as undercut. As a quantitative description of the shape of the etched recess, the etch factor is defined as the value of etched depth divided by the undercut [19]. The etch factor of the TiNi foil was 0.45 which indicates that the slope of the side wall of the etched grooves is less steep, and the edge is not sharp. This will be advantageous for the stent design

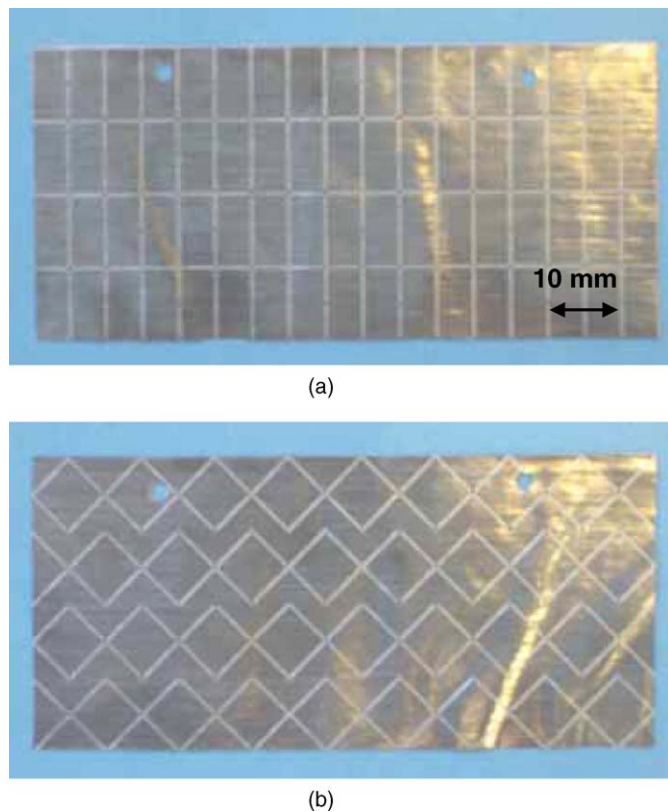


Fig. 4. TiNi foil after etching (a) outer and (b) inner surfaces of the origami stent graft.

because the smooth curvature of the undercut can reduce stress concentration when folded.

### 3.2. Heat treatment

After etching, aging treatment was given to the Ni-rich TiNi foils. One of the reasons for the aging treatment is to set the transformation temperatures close to body temperature as described in Section 2. The other important reason is to store a memory of the cylindrical shape, so that the stent graft would return back to the profile of a cylindrical tube when heated. The foils were constrained by an aluminum tube during the aging (773 K for 20–40 h).

The stent graft after aging treatment is shown in Fig. 5. The foil becomes a cylindrical tube, as expected and designed.



Fig. 5. Origami stent graft (a) projection and (b) side views before folding.

Opposite edges of the foil were connected by adhesive. The diameter and length of the origami stent graft are 25.4 and 40 mm, respectively. The diameter is the same as that of the existing oesophageal or aortal stent grafts.

## 4. Property of self-deployable origami stent graft

### 4.1. Deployment by shape memory effect

The stent graft was cooled below a temperature at  $M_f$  ( $-261$  K) by liquid nitrogen in order to fold it in a fully martensitic state. The folded stent graft was heated by warm air and its deployment was recorded using a digital video camera. A chromel-alumel thermo-couple was attached to the stent graft in order to measure the temperature of the stent graft during deployment.

Figs. 6 and 7 show two series of frames from the video recording of the Ti–50.7 at% Ni SMA stent graft deployment process. Fig. 6 is the side view, whereas Fig. 7 is the end view of the deployment. The stent graft was folded easily and fitted into a small acrylic tube of 13 mm diameter imitating a catheter. The tube was inserted into another acrylic tube of a larger diameter (25 mm) imitating the oesophageal or aorta lumen, see Figs. 6a and 7a, and the stent graft was pushed out from the catheter tube lumen as shown in Figs. 6b and 7b. The inside of the larger diameter tube was pre-heated by warm air above  $A_f = 319$  K before the stent graft was inserted. In addition, the tube was heated from top and bottom during the deployment of the stent graft. As can be seen in Figs. 6 and 7, both length and diameter of the origami stent graft increase gradually. Diameter increases and the expansion is roughly uniform shown in Fig. 7. However, in the middle stage of deployment, it becomes slightly distorted (Fig. 7d and e). It may be a temporary distortion caused by uneven heating of the stent graft. Inside a lumen, a stent graft would be heated relatively evenly, thus uneven heating would be less of a concern.

From the results of the video recordings and temperature measurements by the thermocouple attached onto the stent graft, the relationship between the length, diameter, and the temperature of the stent graft during the deployment can be assessed. Fig. 8(a and b) show the diameter, length, and temperature of the stent graft as a function of heating time. Since, they are measured from separated video recordings, heating rates are slightly dif-

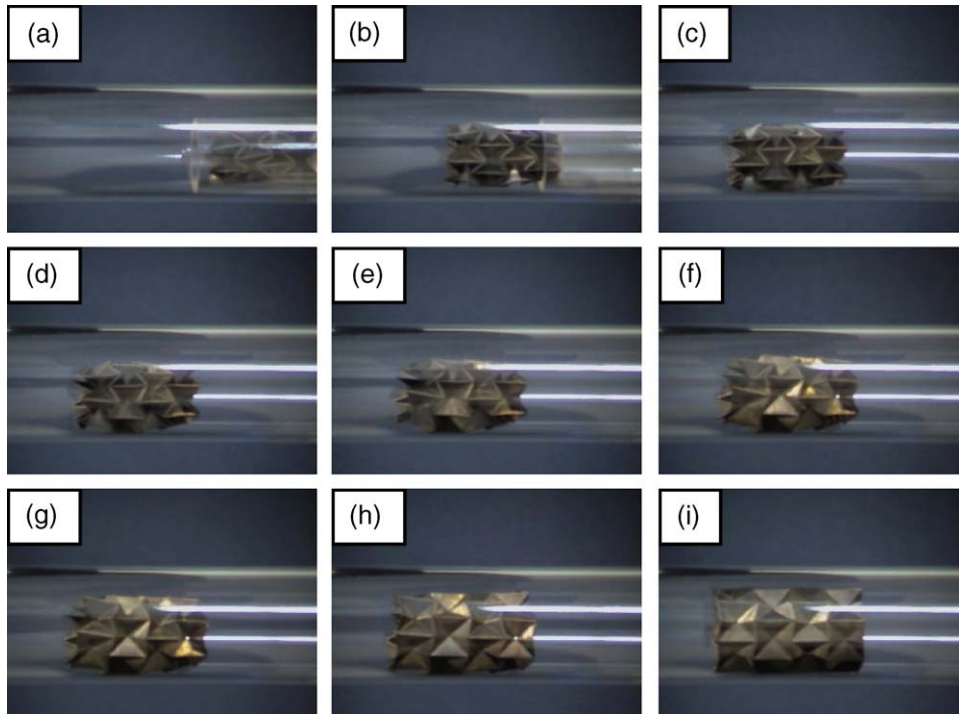


Fig. 6. Series of frames from video recording showing self-deployment of the stent (side view): (a) stent graft which is folded and backed into a small acrylic tube of 13 mm radius was inserted into another acrylic tube of 25 mm radius and (b) the small acrylic tube was removed and (c–i) the stent graft was self-expanding at above  $A_f$  (319 K).

ferent for both cases. Immediately after the small acryl tube (i.e. catheter) was withdrawn, the diameter and length increased by elastic deformation shown by dash lines. They remained constant until the  $A_s$  temperature is reached and then start to increase

gradually by shape memory effect. Increase in length is in accordance with temperature change and reaches the maximum when the temperature reached about 320 K, slightly above a temperature at which the Austenite phase finishes forming,  $A_f$ . This

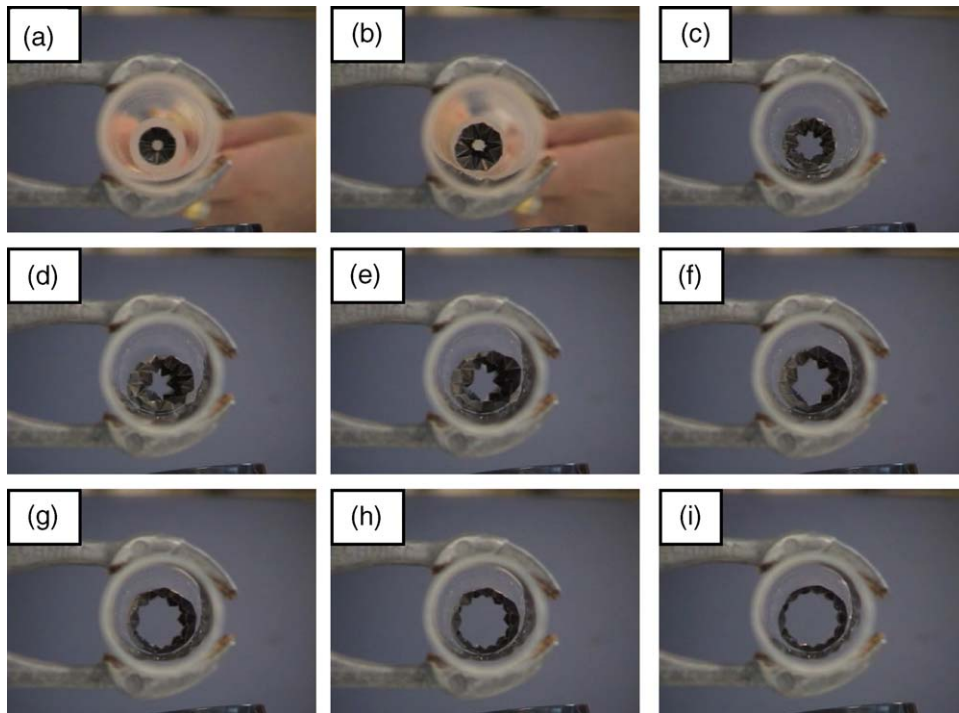


Fig. 7. Series of frames from video recording showing self-deployment of the stent (end view): (a) stent graft which is folded and backed into a small acrylic tube of 13 mm radius was inserted into another acrylic tube of 25 mm radius and (b) the small acrylic tube was removed and (c–i) the stent graft was self-expanding at above  $A_f$  (319 K).

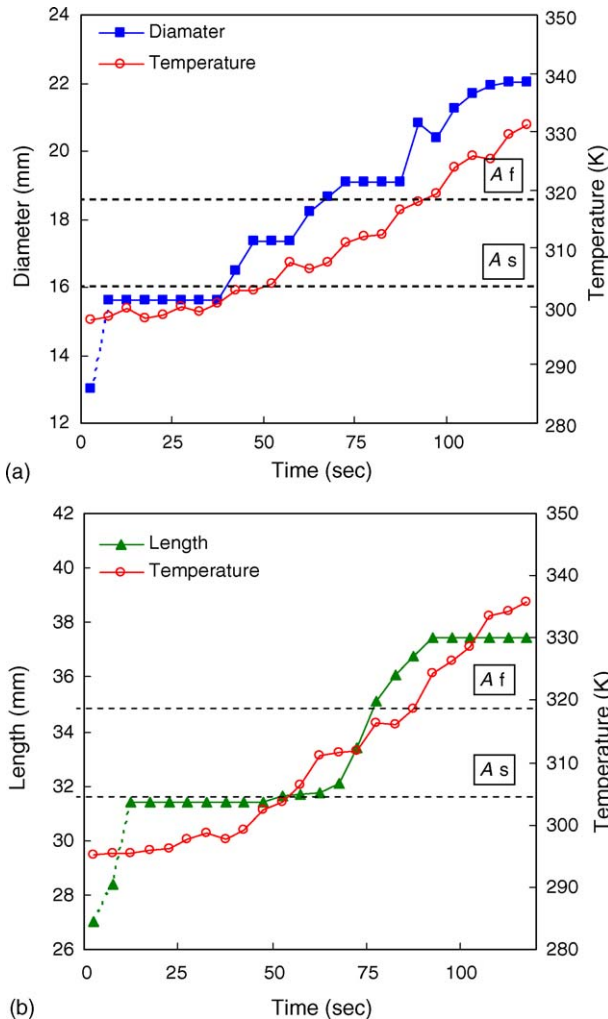


Fig. 8. (a) Diameter and (b) length and temperature vs. heating time.

thermal shape memory effect might be useful to deploy the stent graft without any damages since it deploys gently compared with deployment with superelasticity.

Ratio between the original dimensions and those after shape recovery was 90% and 95% for the diameter and length, respectively, and thus the complete recovery was not achieved. It is due to the fact that the value of the strain at the folds of the stent graft is beyond the recoverable strain which is about 3% for the present foils [14]. Some improvement could be made by modifying the folding pattern, and by adjusting the etching depth and width of the folds.

#### 4.2. Deployment with superelasticity

We also experimented the deployment of the stent graft using superelasticity, as most existing stents do. The stent graft made from Ti–51.3 at% Ni SMA foil was heated above  $A_f$  (312 K), therefore, it behaved superelastically during the experiment. It opened up immediately after the small acryl tube was withdrawn due to release from stress. The deployment was so quick that the video recording was not good enough to catch the deployment process.

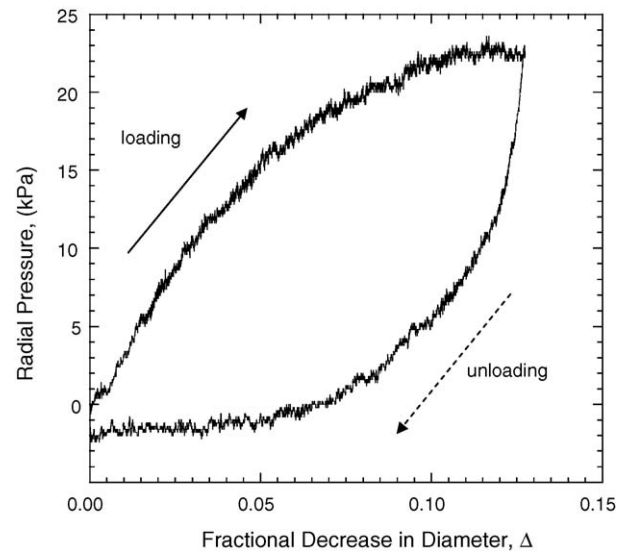


Fig. 9. Load vs. reduction in radius from the result of compression test.

Mechanical property of the stent graft in fully deployed configuration was assessed by a collar test [20]. A strip of vinyl-coated paper was wrapped around the stent graft and a radially inward pressure was applied by pulling both ends of the strip by a universal tensile testing machine. Load was monitored during stressing; the displacement, corresponding to the change in the circumference of the stent graft, was converted into radius change.

Result of the compression test on the stent graft is shown in Fig. 9. The loading force shown by black arrow is much higher than the unloading force shown by black dash arrow, which is typical of superelastic deformation. Therefore, it is found that the stent graft has good resistance against compressive force. This mechanical property is desirable as a stent graft in order to prevent from its collapse for external pressure.

## 5. Conclusions

The working model presented here has shown that the innovative concept of the single piece origami stent graft can be produced using a biocompatible material of the SMA foil made by the newly developed ultrafine laminate method. The good fold patterns have achieved by simple and readily available technique of a negative photochemical etching. The experiments have successfully demonstrated that Ni-rich TiNi SMA stent graft can be deployed at near body temperature or by superelasticity.

We believe that the application of medical device of Ni-rich TiNi SMA foils with deployable structures will be more useful for minimum invasive surgery, such as vascular surgery using an endoscope.

## Acknowledgments

The authors are grateful to Mr. C.W. Band for his assistance in photochemical etching. The research is partially supported by the Japan-U.K. Research Cooperative Program of the Japan Society for the Promotion of Science.

## References

- [1] P.W. Serruys, P. de Jaegere, F. Kiemeneij, C. Macaya, W. Rutsch, G. Heyndrickx, H. Emanuelsson, J. Marco, V. Legrand, P. Materne, *N. Engl. J. Med.* 331 (1994) 489–495.
- [2] A. Adam, R.F. Dondelinger, MPR, *Textbook of Metallic Stents*, ISIS Medical Media, Oxford, 1997.
- [3] B.L. Dolmatch, U. Blum, *Stent-Grafts/Current Clinical Practice*, Thieme, New York, 2000.
- [4] M.G. Cowling, *Hosp. Med.* 61 (2000) 33–36.
- [5] E.R. Edelman, C. Rogers, *Circulation* 94 (1996) 1199–1202.
- [6] M. Gottsauner-Wolf, D.J. Moliterno, A.M. Lincoff, E.J. Topol, *Clin. Cardiol.* 19 (1996) 347–356.
- [7] T.A. Chuter, *Cardiovasc. Surg.* 10 (2002) 7–13.
- [8] T.S. Jacobs, J. Won, E.C. Gravereaux, P.L. Faries, N. Morrissey, V.J. Teodorescu, L.H. Hollier, M.L. Marin, *J. Vasc. Surg.* 37 (2003) 16–26.
- [9] K. Kuribayashi, Y. Zhong, U.K., US, EU and Japan Patent PCT/GB02/01424, 2002.
- [10] T. Duerig, A. Pelton, D. Stockel, *Mater. Sci. Eng. A* 273–275 (1999) 149–160.
- [11] D. Stoeckel, *Minim. Invasive Ther. Allied Technol.* 9 (2000) 81–88.
- [12] W. Moorlegghem, V.M. Chandrasekaran, D. Reynaerts, J. Peirs, H.V. Brussel, *Biomed. Mater. Eng.* 8 (1998) 55–60.
- [13] J. Ryhanen, Biocompatibility evaluation of nickel–titanium shape memory metal alloy, in: *Dissertation*, University Hospital of Oulu, Oulu, 1999.
- [14] D. Tomus, K. Tsuchiya, M. Inuzuka, M. Sasaki, D. Imai, T. Ohmori, M. Umemoto, *Scr. Mater.* 48 (2003) 489–494.
- [15] I. Gotman, *J. Endourol.* 11 (1997) 383–389.
- [16] T. Saburi, Ti–Ni shape memory alloys, in: K. Otsuka, C. Wayman M (Eds.), *Shape Memory Materials*, Cambridge University Press, Cambridge, UK, 1998, pp. 49–96.
- [17] M. Kohl, E. Quandt, A. Schubler, R. Trapp, Characterization of NiTi shape memory microdevices produced by microstructuring of etched sheets or sputter deposited films, in: *Fourth International Conference on New Actuators*, 1994, pp. 317–320.
- [18] D. Reynaerts, J. Peirs, H.V. Brusse, Design of a shape memory actuated gastrointestinal intervention system, in: *Fifth International Conference on New Actuators*, 1996, pp. 409–412.
- [19] D.M. Allen, *The Principles and Practice of Photochemical Machining and Photoetching*, Adam Hilger, 1986.
- [20] C.M. Agrawal, H.G. Clark, *Invest. Radiol.* 27 (1992) 1020–1024.